








Article

Bioengineered Flagellin–TiO₂ Nanoparticle-Based Modified Glassy Carbon Electrodes as a Highly Selective Platform for the Determination of Diclofenac Sodium

Juan Santiago Hidalgo ^{1,2} , Éva Tóth ³ , Hajnalka Jankovics ^{3,†} , Carmen Ioana Fort ² , Graziella Liana Turdean ^{2,*} ,
Etelka Tombacz ^{3,†}  and Ildiko Galambos ¹ 

- ¹ Soós Ernő Research and Development Center, University of Pannonia, Zrínyi Miklós St. 18, H-8800 Nagykanizsa, Hungary; juansannin2595@gmail.com (J.S.H.); galambos.ildiko@pen.uni-pannon.hu (I.G.)
- ² Research Center of Electrochemistry and Non-Conventional Materials, Department of Chemical Engineering, Faculty of Chemistry and Chemical Engineering, “Babes-Bolyai” University, Arany Janos St. 11, 400028 Cluj-Napoca, Romania; iladiu@chem.ubbcluj.ro
- ³ Bio-Nanosystems Laboratory, Research Institute of Biomolecular and Chemical Engineering, University of Pannonia, Egyetem St. 10, H-8200 Veszprém, Hungary; toth.eva@mk.uni-pannon.hu (É.T.); jankovics.hajnalka@mk.uni-pannon.hu (H.J.); tombacz.etelka@pen.uni-pannon.hu (E.T.)
- * Correspondence: graziella.turdean@ubbcluj.ro
- † These authors contributed equally to this work.

Abstract: This study describes the incorporation of bioengineered flagellin (4HIS) protein in conjunction with TiO₂ anatase nanoparticles into a chitosan (Chit) polymeric matrix as a highly sensitive electrode modifier for the determination of diclofenac sodium (DS) in wastewater. Two types of electrodes were prepared using a simple drop-casting method. The inner structure of the obtained modified electrode was characterized by scanning electron microscopy (SEM) in combination with energy-dispersive X-ray spectroscopy and isothermal titration calorimetry (ITC). The electrochemical and electroanalytical parameters of DS oxidation at the nanostructured interface of the modified electrode were obtained via cyclic voltammetry and square-wave voltammetry. The analytical parameters for diclofenac electro-detection showed a 50% decrease in LOD and LOQ at Chit + TiO₂ + 4HIS/GCE-modified electrode compared with the Chit + 4HIS/GCE-modified electrode. The obtained tools were successfully used for DS detection in drug tablets and wastewater samples. Thus, it was demonstrated that in the presence of a histidine-containing flagellin variant, the electrode has DS recognition capacity which increases in the presence of TiO₂ nanoparticles, and both induce excellent performances of the prepared tools, either in synthetic solution or in real samples.

Keywords: biosensor; flagellin; TiO₂ nanoparticles; cyclic voltammetry; square-wave voltammetry; electrochemical impedance spectroscopy; diclofenac sodium; wastewater



Citation: Hidalgo, J.S.; Tóth, É.; Jankovics, H.; Fort, C.I.; Turdean, G.L.; Tombacz, E.; Galambos, I. Bioengineered Flagellin–TiO₂ Nanoparticle-Based Modified Glassy Carbon Electrodes as a Highly Selective Platform for the Determination of Diclofenac Sodium. *Chemosensors* **2023**, *11*, 576. <https://doi.org/10.3390/chemosensors11120576>

Academic Editor: Núria Serrano

Received: 31 October 2023

Revised: 22 November 2023

Accepted: 28 November 2023

Published: 7 December 2023



Copyright: © 2023 by the authors. Licensee MDPI, Basel, Switzerland. This article is an open access article distributed under the terms and conditions of the Creative Commons Attribution (CC BY) license (<https://creativecommons.org/licenses/by/4.0/>).

1. Introduction

Human and veterinary pharmaceutical residue, especially diclofenac sodium (DS), often arrives in the aquatic ecosystem, leading to direct toxicological consequences on humans, the long-term (chronic) exposure being reported to have effects worldwide [1]. In this context, diclofenac was included in the first Watch List of the Water Framework Directive with a predicted no-effect concentration of 50 ng/L (i.e., 0.17 nM) [2,3].

Diclofenac sodium (DS, 2-(2-((2,6-dichlorophenyl)amino)phenyl)acetic acid) is a non-steroidal anti-inflammatory drug (NSAID), having antipyretic and analgesic properties, often used to reduce inflammation and certain types of pain.

Given the importance of DS in groundwater and the European Union legislation, numerous techniques have been employed to determine DS, including chromatography (i.e., gas chromatography–mass spectrometry [4,5], liquid chromatography [6–8], liquid

chromatography–mass spectrometry [9], thin layer chromatography [10], spectrophotometry [11–15], colorimetry [16], spectrofluorimetry [17], and capillary zone electrophoresis (CZE) [18].

These methods are time-consuming and/or expensive (e.g., specialized equipment, highly skilled operators, and the use of high-purity reagents and standards) and often need the sample pretreatment step. To overcome these drawbacks, electrochemical methods based on chemically modified electrodes [18–22] are used extensively for their properties such as selectivity, reproducibility, low cost, and simplicity [18–23]. DS determination via electrochemical methods was reported in the literature, using either unmodified electrodes (e.g., edge plane pyrolytic graphite electrode [24]), or modified electrodes, using as modifiers metal or metal oxide nanomaterials [25,26], carbon nanomaterials (e.g., carbon nanotubes [27], graphene [28]), conducting polymers [29], ionic liquids (ILs), inorganic complexes (e.g., nickel hydroxide-modified nickel electrode [30]), etc.

In order to enhance the selectivity of the modified electrode, engineered biological macromolecules immobilized on a modified electrode surface can be an efficient alternative for drug determination. Proteins of large size and varied composition are particularly suitable for developing highly specific sensing materials into biosensors due to their complex structure and interaction pattern. Thus, for example, flagellin-based proteins able to build long (up to 10 μm), highly stable filaments from thousands of monomer units by self-assembly can be modified to have a great specificity for binding a certain contaminant [31]. The redox process facilitated by the presence of a designed protein immobilized at the electrode surface is often mediated by the presence of nanomaterials, resulting in improved electroanalytical performance of the device. [32].

Nanotechnology and nanomaterials have received a lot of attention in electrode development in recent years due to their positive impacts on analytical performances such as increased sensitivity, selectivity, and repeatability, which are due to the low density, high porosity, specific surface area, surface-to-volume ratio, reactivity, biocompatibility, and adsorption capacity of used nanocomposites [33,34]. TiO_2 nanoparticles are catalytically active electrode materials [35], having a porous structure that preserves the nano-architecture of an interconnected nanoparticle porous network [36]. Also, as a result of its other unique properties (i.e., good conductivity, high surface area, high porosity, strong adsorptive capability, chemical inertness, optical transparency, chemical/thermal stability, non-toxicity, and good biocompatibility), it has a high potential for use as modifying agents for electrode materials. [36,37].

Furthermore, when compared to solid graphite or noble metal electrodes, TiO_2 nanoparticle-based electrodes have a reduced background current. Other advantages include a larger potential window, improved stability, and increased repeatability. Consequently, TiO_2 nanoparticles can be combined with other compounds (such as graphite, carbon nanotubes, etc.), and the synergistic effect leads to a significant improvement in electrode performance (due to an increase in both surface electroactive area and electron transfer rate between the electrode and the target molecule) [35].

Based on these advantages, the aim of this paper was to combine bioengineered flagellin (4HIS) protein with TiO_2 nanoparticles immobilized via an eco-friendly polymer (chitosan) in order to create, for the first time, to our knowledge, a novel modified electrode useful for a more specific determination of DS. The modified electrode prepared via the drop-casting method was electrochemically characterized by cyclic voltammetry, square-wave voltammetry, and electrochemical impedance spectroscopy. The developed modified electrode demonstrated a good detection limit, linear range, and selectivity, being successfully applied for the determination of DS in drug tablets and wastewater samples.

2. Materials and Methods

2.1. Materials and Reagents

The following reagent were used: acetic acid (0.1 molar, $\text{C}_2\text{H}_4\text{O}_2$, “Reactivul” Bucuresti), chitosan ($\text{C}_{12}\text{H}_{24}\text{N}_2\text{O}_9$, from crab shells, Sigma-Aldrich, St. Louis, MO, USA),

disodium phosphate ($\text{Na}_2\text{HPO}_4 \cdot 12\text{H}_2\text{O}$, 99% pure, "Reactivul" Bucuresti), potassium phosphate monobasic (KH_2PO_4 , 99.5% pure, Sigma Aldrich), phosphoric acid (H_3PO_4 , 0.1 M, Sigma-Aldrich), potassium hexacyanoferrate(III) ($\text{K}_3[\text{Fe}(\text{CN})_6]$, 99% pure, Fein-biochemica, Bucuresti), potassium ferrocyanide ($\text{K}_4[\text{Fe}(\text{CN})_6 \cdot \text{H}_2\text{O}$, 99% pure, Chimopat, Bucuresti), diclofenac sodium (DS, $\text{C}_{14}\text{H}_{10}\text{Cl}_2\text{NNaO}_2$, 99% pure, Sigma-Aldrich), glucose monohydrate ($\text{C}_6\text{H}_{12}\text{O}_6 \cdot \text{H}_2\text{O}$, 99% pure, Merck, Darmstadt, Germany), citric acid monohydrate ($\text{C}_6\text{H}_8\text{O}_7 \cdot \text{H}_2\text{O}$, 99% pure, Sigma Aldrich), fructose ($\text{C}_6\text{H}_{12}\text{O}_6$, 99% pure, Sigma Aldrich), Ibuprofen ($\text{C}_{13}\text{H}_{18}\text{O}_2$, Sun Pharma, Cluj-Napoca, Romania), paracetamol ($\text{C}_8\text{H}_9\text{NO}_2$, Sun Pharma, Cluj-Napoca), dopamine hydrochloride ($\text{C}_8\text{H}_{11}\text{NO}_2$, 99%, Alfa Aesar, Ward Hill, MA, USA), sodium hydroxide (NaOH, 85% pure, Merck), potassium chloride (KCl, 99% pure, "Reactivul" Bucuresti), titanium oxide anatase (TiO_2 , anatase, 99.5%, particle size 10–30 nm, Sigma Aldrich), ethanol (98% pure, "Reactivul", Bucuresti). Diclofenac tablets (50 mg, from Rambaxy-Terapia, Cluj-Napoca, Romania) were purchased from a local pharmacy.

A suspension of a 4HIS flagellin variant in polymeric form was prepared in the laboratory of the Research Institute of Biomolecular and Chemical Engineering (Veszprem, Hungary) according to [37], except that polymer formation was performed in 20 mM 4-(2-hydroxyethyl)-1-piperazine ethanesulfonic acid (HEPES) (Sigma-Aldrich), 150 mM NaCl, and pH 7.0 buffer, via the addition of ammonium sulfate in a final concentration of 0.6 M.

The phosphate buffer solution (PB, 0.025 M, pH 4.6) was prepared by dissolving the appropriate amount of $\text{Na}_2\text{HPO}_4 \times 12 \text{H}_2\text{O}$ and KH_2PO_4 in distilled water [38]. A 0.1 M DS stock solution was prepared in buffer solution and stored at 4 °C in the refrigerator.

Diluted H_3PO_4 and NaOH solutions were used for adjusting the pH of the buffer solutions. All chemicals having analytical purity were used as received, without any purification.

2.2. Characterization Technique

The morphological structure of the prepared biosensor was carried out using a scanning electron microscope (VEGAS 3 SBU, Tescan, Brno–Kohoutovice, Czech Republic), which was equipped with a primary and secondary electron detector, to observe the inner part of the sample. Furthermore, the scanning electron microscopy (SEM) was equipped with spectra of energy-dispersive X-ray spectroscopy (EDXS), and chemical maps for the elements were acquired using a Dual EDX System (Bruker, Karlsruhe, Germany).

Isothermal titration calorimetry (ITC) experiments were carried out at 25 ± 0.2 °C by a MicroCal PEAQ-ITC calorimeter. Due to the low solubility of DS at pH 4.6, ITC measurements were performed at pH 7.0. A 5 mg/mL solution of the 4HIS flagellin variant in monomeric form was prepared in 100 mM HEPES and 150 mM NaCl (pH 7.0). The diclofenac Na salt solution was prepared in final volumes of 10 mL (1.35 mM) and 5 mL (6.475 mM) via direct volumetric adjustment with the same buffer to volume. In all cases, the diclofenac solution was titrated into the protein at the end point of titration in molar excesses of 2.2 (monomeric only) and 11-fold (monomeric and polymeric protein). The ITC data were fitted to a one-binding-site model with the MicroCal PEAQ-ITC Analysis Software package provided by MicroCal, using a non-linear least-squares algorithm.

2.3. Preparation of the Modified Electrode

The glassy carbon electrode (inner diameter of 3 mm, from ALS Co., Tokyo, Japan) was polished on felt material with alumina slurry (0.3 μm , Buehler, Crissier, Switzerland). After that, it was placed in distilled water in ultrasound equipment for 10 min and then was thoroughly rinsed with ethanol and distilled water.

The 0.1 % chitosan solution was prepared via sonication for 30 min, with 10 mg chitosan in 10 mL of 0.1 M acetic acid. A suspension containing 1 μL 4HIS (corresponding to 2 μg flagellin) and 1 mg TiO_2 anatase in 1 mL chitosan solution was sonicated for 3 h.

Electrode modification via the drop-casting method consists of depositing three times a volume of 3 μL of the above-prepared suspension onto the clean GCE surface and drying

it at room temperature via slow solvent evaporation for 2 h. Thus, the obtained electrodes were symbolized as Chit/GCE, Chit + 4HIS/GCE, and Chit + TiO₂ + 4HIS/GCE.

2.4. Electrode Characterization

The electrochemical characterization of the prepared modified electrodes was performed using a computer-controlled AutoLab potentiostat (PGSTAT302N and PGSTAT 12, EcoChemie, Utrecht, The Netherlands) operated by GPES 4.7 software for cyclic voltammetry (CV) and square-wave voltammetry (SWV) measurements. A conventional three-electrodes cell, equipped with a working GC-modified electrode, an Ag/AgCl, KCl_{sat} reference electrode, and a platinum plate auxiliary electrode, was connected to the potentiostat.

2.5. Analysis of the Water Sample

To demonstrate the real application perspective of the performed modified electrode, a real water sample was collected from the city's wastewater treatment plant (Cluj Napoca, Romania) and analyzed using the standard addition method. The wastewater sample was used as it was obtained, without any pretreatment. Also, an HPLC-MS analysis was performed on the wastewater samples (SOOS laboratory, Nagykanizsa, Hungary) to compare the sensor's results.

3. Results

3.1. Morpho Structural Characterization of GCE-Modified Electrodes

The morphological characterization of the films deposited on the GC surface was performed using SEM and is presented in Figure 1A,B. The Chi + 4HIS coating displays a slightly rough surface (Figure 1A) without noticeable cracks along the electrode surface.

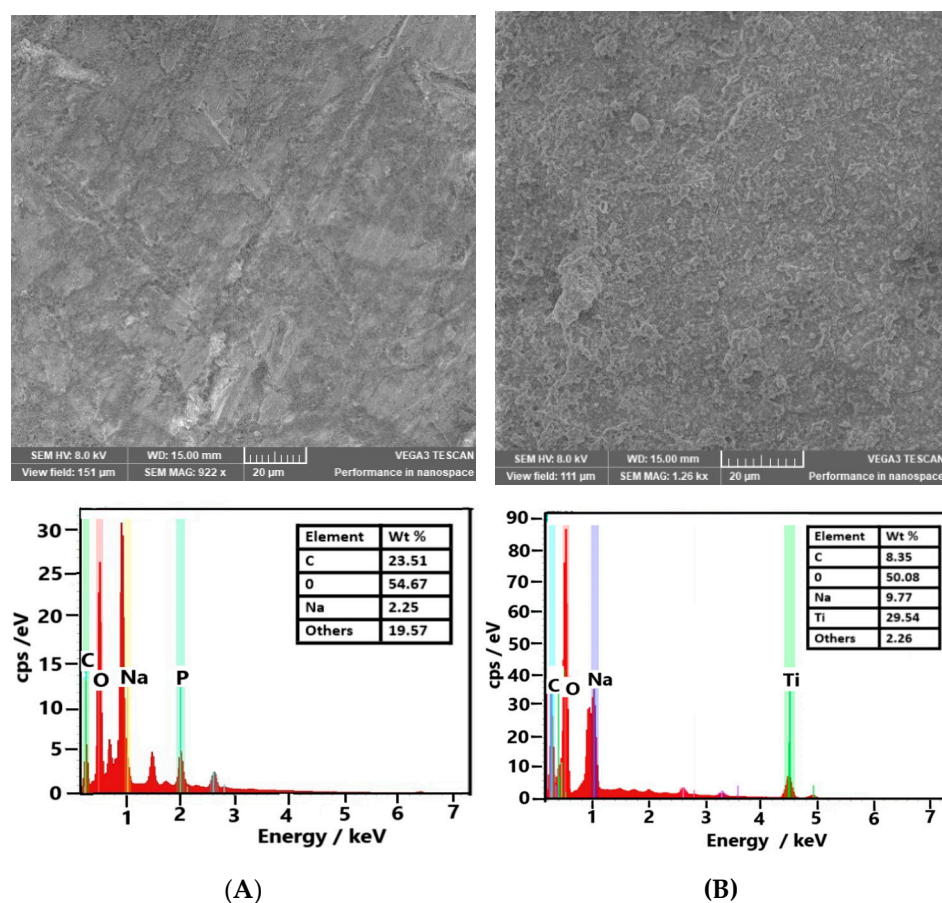


Figure 1. SEM images of Chit + 4HIS (A) and Chit + TiO₂ + 4HIS (B) samples and the corresponding EDX spectra indicating the film composition.

The Chi + TiO₂ + 4HIS coating is much thicker, and a dense arrangement of submicron-sized clumps appears to uniformly cover the entire electrode surface (Figure 1B). In contrast to a uniform planar structure of the Chit, some agglomerations can be seen in the presence of 4HIS and TiO₂ surfaces. From EDX spectra, the presence of Ti is confirmed in the samples containing TiO₂, proving its immobilization which occurs during the preparation of the modifier film.

3.2. Electrochemical Behavior of GCE-Modified Electrodes for DS Detection

The electrochemical characteristics of the prepared modified electrode were evaluated by cyclic voltammetry. At 50 mV·s⁻¹ (Figure 2), the DS oxidation peak is not visible at the Chit/GCE-modified electrode, while the DS well-defined irreversible oxidation peak is placed at 0.763 V vs. Ag/AgCl, KCl_{sat} at the Chit + 4HIS/GCE-modified electrode and is shifted in the presence of TiO₂ nanoparticles to a lower value of 0.698 V vs. Ag/AgCl, KCl_{sat} at Chit + TiO₂ + 4HIS/GCE-modified electrodes. DS oxidation is an irreversible process, as no cathodic peak is recorded. Similar values have been reported in the literature [39–42]. Also, the oxidation peak current intensity increases from 4.11 × 10⁻⁶ A at Chit + 4HIS/GCE to 7.01 × 10⁻⁶ A at Chit + TiO₂ + 4HIS/GCE, respectively. This means that there is an increase in current intensities of 70% in the presence of TiO₂ in the modified matrix of the electrode, demonstrating the electrocatalytic performance effect of the TiO₂ anatase nanoparticles.

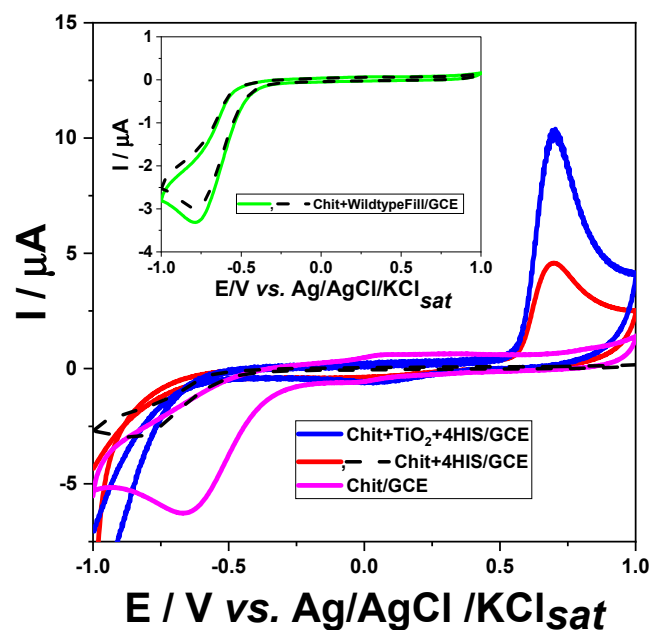


Figure 2. Cyclic voltammograms in the absence (black dash line) and in the presence of 10⁻³ M diclofenac in 0.025 M PB (pH 4.6) at different modified electrodes (see inset, colored solid line). Experimental conditions: scan rate, 50 mV·s⁻¹; starting potential, -1 V vs. Ag/AgCl, KCl_{sat}.

Based on the above, the detection of DS is clearly associated with the presence of 4HIS flagellin among the electrode surface components. To understand this more thoroughly, isothermal titration calorimetry was used. ITC measurements of the polymer and monomer 4HIS at pH 7 (due to solubility problems of DS at a lower pH) showed no interaction with DS even at 10-fold molar excess. This is in agreement with our previous observation that the 4HIS flagellin variant specifically binds Ni(II) at a neutral pH [43]. In addition, it was observed that the wild-type flagellin-containing electrode (Chit + wild-type Fill/GCE) did not exhibit an oxidation peak, indicating that the non-modified filaments were unable to detect diclofenac sodium. The 4HIS flagellin was constructed from the wild-type with the modification of L209H-V235H-K241H-S264H, suggesting that the role of the protein in DS

detection can be reduced to its histidine side chains. ITC titrations suggest that when the protein is properly folded, the buried binding pocket formed by the four histidine side chains is not accessible to DS. However, the electrode was prepared in 0.1 M acetic acid solution (pH~2.9) by stirring for 3 h, which is likely to lead to the decomposition of the starting polymer and unfolding of the monomers. With the unfolding of the 4HIS, the binding pocket is eliminated, and the histidine side chains can be positioned on the protein surface, accessible to DS. As well, the behavior of the Chit + TiO₂ + 4HIS/GCE electrode could be explained by the synergetic effect of the biochemical arrangement of 4HIS in recognizing DS in the solution and of the spatial distribution of the TiO₂ nanoparticles in the modified electrode matrix, which increases the electrochemically active surface area of the electrode matrix.

In order to estimate the electrochemical active area, CVs were performed in a scan rate range of 0.010–1 V s⁻¹ in a solution of 0.1 M KCl containing 0.5 mM of K₃[Fe(CN)₆]/K₄[Fe(CN)₆. For both studied modified electrodes, an increase in the anodic peak current intensities (*I*_{p,a}) and the scan rate (*v*) was observed (Figure 3A,B).

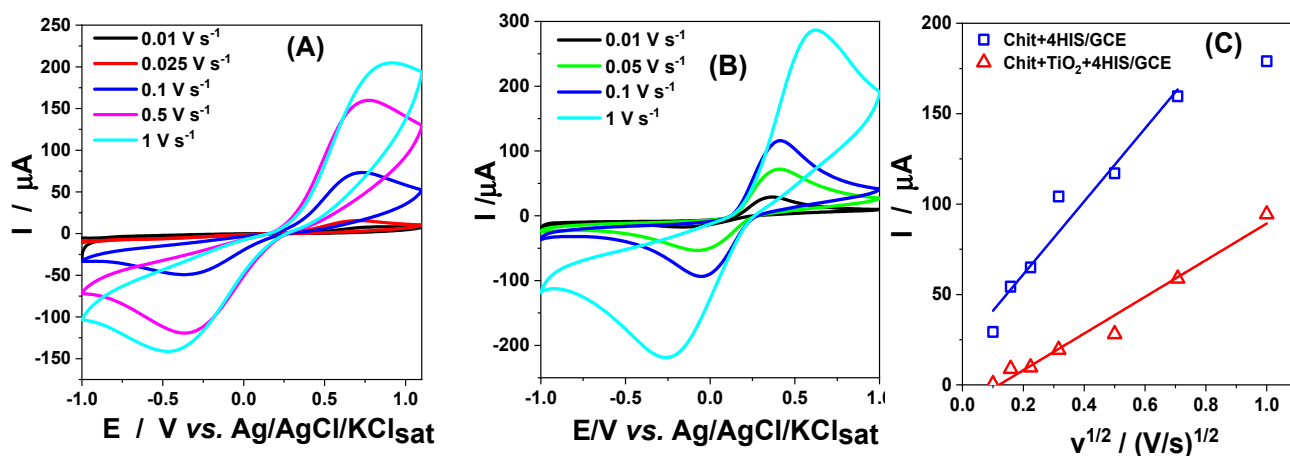


Figure 3. Cyclic voltammograms at Chit + 4HIS/GCE (A) and Chit + TiO₂ + 4HIS/GCE (B)-modified electrodes in 0.1 M KCl containing 0.5 mM K₃[Fe(CN)₆]/K₄[Fe(CN)₆ solution and the corresponding *I* versus *v*^{1/2} dependencies (C). Experimental conditions: scan rates, see inset; starting potential, −1 V vs. Ag/AgCl, KCl_{sat}.

The electrode process, involving the redox couple [Fe(CN)₆]^{3−}/[Fe(CN)₆]^{4−}, is a quasi-reversible one-electron transfer process which obeys the Randles–Ševčík Equation (1) [44]:

$$I_{p,a} = (2.69 \times 10^5) n^{3/2} \cdot A \cdot C_0 \cdot D^{1/2} \cdot v^{1/2} \quad (1)$$

where *I*_{p,a} is the anodic peak current (in A), *n* is the number of electrons transferred (in our case, one electron for the [Fe(CN)₆]^{3−}/[Fe(CN)₆]^{4−} redox couple), *A* is the active surface area of the electrode (in cm²), *C*₀ is the concentration of the solution (in mol/cm³; in our case, 0.5 × 10^{−6} mol/cm³), *D* is the diffusion coefficient (cm²·s^{−1}; in our case, 7.60 × 10^{−6} cm²·s^{−1} [45]), and *v* is the scan rate (in V/s).

The obtained linear dependences between *I* versus *v*^{1/2} are as follows (Figure 3C):

$I/A = (-1.21 \times 10^{-5} \pm 3.81 \times 10^{-6}) + (1.01 \times 10^{-4} \pm 7.24 \times 10^{-6})v^{1/2}/(V/s)^{1/2}$, *R*/no. points = 0.9875/7, for Chit + 4HIS/GCE;

$I/A = (2.08 \times 10^{-5} \pm 9.08 \times 10^{-6}) + (2.02 \times 10^{-4} \pm 2.3 \times 10^{-5})v^{1/2}/(V/s)^{1/2}$, *R*/no. points = 0.9750/6, for Chit + TiO₂ + 4HIS/GCE.

Using the slope value of *I* versus *v*^{1/2} dependencies and Equation (1), for the active surface area, the values obtained were 0.136 cm² for Chit + 4HIS/GCE and 0.272 cm² for Chit + TiO₂ + 4HIS/GCE-modified electrodes, respectively. Compared with the geometric area of the electrode of 0.07065 cm², the active surface area of the modified electrodes is

greater. Also, it must be pointed out that the presence of TiO_2 increases the active surface area of the electrode twice, as expected.

3.2.1. Influence of Scan Rate on DS Oxidation

Figure 4A shows the influence of the scan rate on DS oxidation at the Chit + 4HIS + TiO_2 /GCE-modified electrode. As expected, the peak potential shifted to a more positive value of potential with the increase in the scan rate. The following linear log I versus log v dependencies were obtained:

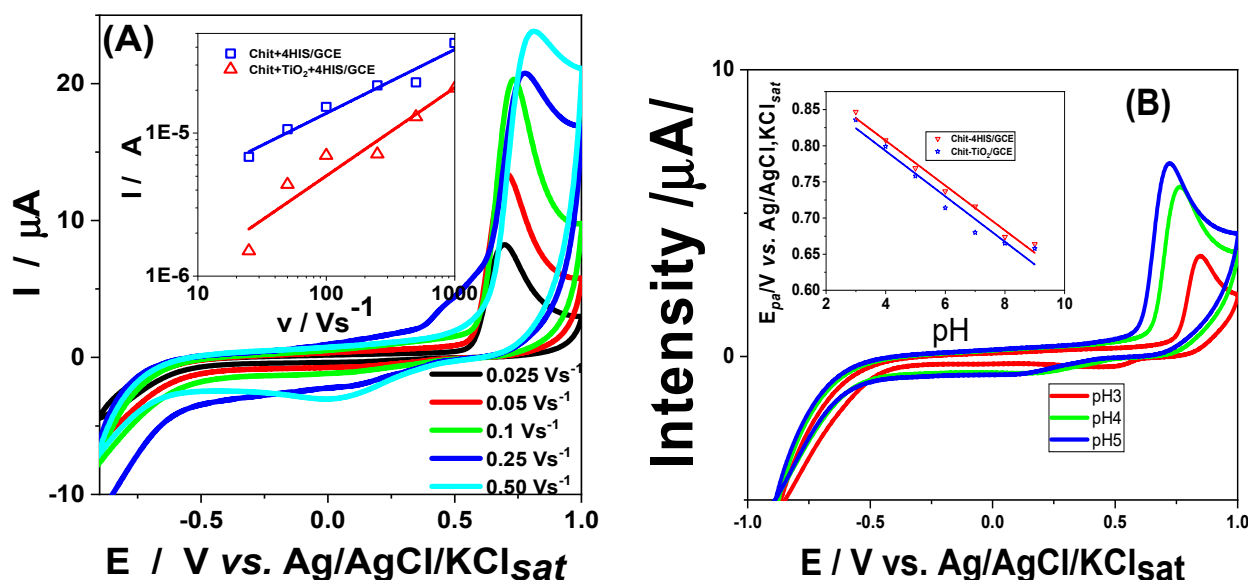


Figure 4. Influence of the scan rate on the cyclic voltammograms of 10^{-3} M DS at Chit + 4HIS + TiO_2 /GCE-modified electrode. Inset: log I vs. log v dependencies for different modified electrodes (see inset) (A). Influence of pH on the peak potential of 10^{-3} M DS oxidation (B). Experimental conditions: electrolyte, 0.025 M PB (pH 4.6); starting potential, -1 V vs. Ag/AgCl, KCl_{sat} .

$\log I/A = (-6.53 \pm 0.218) + (0.618 \pm 0.095) \log v/(V/s)$, $R/\text{no. points} = 0.9550/6$, for Chit + 4HIS/GCE;

$\log I/A = (-5.76 \pm 0.103) + (0.447 \pm 0.046) \log v/(V/s)$, $R/\text{no. points} = 0.9799/6$, for Chit + TiO_2 + 4HIS/GCE.

The slopes of log I vs. log v dependencies (Figure 4A inset) with values close to 0.5 are characteristic of redox processes controlled by diffusion, while values close to 1 indicate processes controlled by adsorption [44]. From the data in the previous equations, it can be concluded that the redox process at the electrode occurred under diffusion control in both cases of modified electrodes.

3.2.2. Influence of the pH on DS Oxidation

It is worth mentioning that the pH of the electrolyte could have an important impact on the catalytic properties of the modifier and thus on its behavior, the reaction mechanism at the electrode, and the analytical parameters of the modified electrode. In this context, the effect of the pH of the supporting electrolyte in the range of 3.0–8.0 on the electrooxidation of 10^{-3} M DS at different modified GCEs was studied using cyclic voltammetry at a scan rate of 50 mV s^{-1} (Figure 4B). It can be observed that the anodic peak potential values gradually shift to more negative potential values as the pH increases. This behavior suggests that protons are involved in the oxidation reaction at the electrode interface [45,46].

The linear dependencies of the anodic peak potential on pH have the following slopes: -0.033 ± 0.003 ($R/n = 0.9935/5$) at Chit + 4HIS/GCE and -0.040 ± 0.001 ($R/n = 0.9993/5$) at Chit + TiO_2 + 4HIS/GCE, respectively. Those values show a slight sub-Nernstian

behavior compared to the theoretical Nernstian slope of 0.059 V/pH. This action is probably due to the bioengineered flagellin (4HIS) protein component of the electrode matrix, whose behavior is influenced by the variation in pH.

3.3. Analytical Characterization

For the analytical detection of diclofenac, the square-wave voltammetry (SWV) method was used due to its high sensitivity, enhanced peak resolution, and ability to discriminate the capacitive current [47] or to have low background current [48]. Figure 5A presents, as an example, the voltammograms recorded at the Chit + TiO₂ + 4HIS/GCE-modified electrode, and the calibration curves for all modified electrodes are presented in Figure 5B.

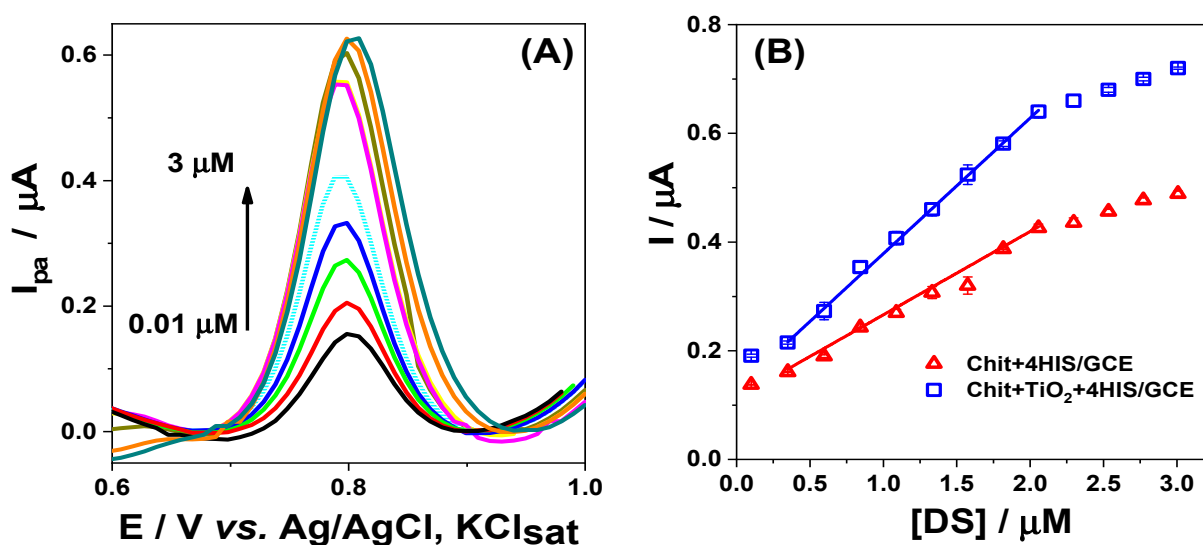


Figure 5. SWVs recorded at Chit + TiO₂ + 4HIS/GCE (A) and the corresponding calibration curves for different modified electrodes (see inset) (B). Experimental conditions: electrolyte, 0.025 M PB (pH 4.6); stock solution, 10^{−4} M DS; frequency, 10 Hz; step potential, 0.01 V; amplitude, 0.01 V; starting potential, 0.6 V vs. Ag/AgCl, KCl_{sat}.

Linear dependencies between the anodic peak current intensities and DS concentrations were obtained in the concentration ranges from 0.25 × 10^{−6} to 2 × 10^{−6} M DS and 0.11 × 10^{−6} to 2 × 10^{−6} M DS at Chit + 4HIS/GCE and Chit + TiO₂ + 4HIS/GCE-modified electrodes, respectively, as described by the following regression equations:

$$I_{p,a}/A = (1.13 \times 10^{-7} \pm 3.87 \times 10^{-9}) + (0.153 \pm 0.004) [DS]/M, R = 0.9976 \text{ n} = 8 \text{ points, at Chit + 4HIS/GCE;}$$

$$I_{p,a}/A = (1.29 \times 10^{-7} \pm 2.42 \times 10^{-9}) + (0.250 \pm 0.003) [DS]/M, R = 0.9997, \text{ n} = 8 \text{ points, at the Chit + TiO}_2 + 4\text{HIS/GCE-modified electrode, respectively.}$$

When compared to the Chit+4HIS/GCE-modified electrode, the sensitivity of the Chit + TiO₂ + 4HIS/GCE-modified electrode is about twice as high. The limits of detection (LOD) and the limit of quantification (LOQ) were calculated as 3 × s_b/m, and 10 × s_b/m, where s_b is the standard deviation blank analyte signal and m is the slope of the calibration equation [49]). The obtained values of LOD were 0.066 μM and 0.033 μM DS, and 0.252 μM and 0.111 μM DS for LOQ, at Chit + 4HIS/GCE and Chit + TiO₂ + 4HIS/GCE-modified electrodes, respectively. As seen, a 50% lower LOD and LOQ were obtained for the Chit + TiO₂ + 4HIS/GCE-modified electrode in comparison with the Chit + 4HIS/GCE-modified electrode, proving the beneficial effect of the presence of TiO₂ in the modifier matrix of the electrode. The obtained LOD values are comparable [29] or even better [20,25,26,39,40,50] than those obtained for quasi-similar sensors reported in the literature (Table 1).

Table 1. Comparison of the electroanalytical performances of the different modified electrodes for the determination of DS.

Electrode	LOD (μM)	Linear Range (μM)	Real Sample	References
GO-COOH/GCE	0.09	1.2–400	/	[20]
Au–Pt NPs/f-MWCNTs/Au	0.30	0.5–1000	/	[25]
CeO ₂ NPs/SPCE	0.40	0.1–26	Tablets	[26]
nanoTiO ₂ /PEDOT/GCE	0.03	4–15	/	[29]
Amino-labeled	0.27	5–1000	Blood serum	[39]
aptamer/Fe ₃ O ₄ /AuNP/CNT/GCE	20	10^{-5} – 1.3×10^{-3}	Tap and surface water	[40]
NiNPs/erGO/GCE	0.09	0.25–125	/	[50]
Chit + 4HIS/GCE	0.066	0.25–2	Wastewater	This work
Chit + TiO ₂ + 4HIS/GCE	0.033	0.11–2	Wastewater	This work

SPCE = graphite-based screen-printed carbon electrodes; AuNPs = gold nanoparticles (AuNPs); CNT = carbon nanotubes; GO-COOH/GCE = carboxyl-functionalized graphene oxide; Au–Pt NPs/f-MWCNTs/Au = Au–Pt nanoparticles (Au–Pt NPs) and functionalized multiwalled carbon nanotubes (f-MWCNTs); PEDOT = poly(3,4-ethylenedioxythiophene); erGO = electrochemically reduced graphene oxide.

The repeatability and reproducibility of the modified electrodes were investigated by recording the square-wave voltammograms for 3 μM DS in 0.025 M PB solution (pH 4.6). The repeatability was examined using the same electrode for six consecutive measurements, obtaining a relative standard deviation (RSD) of the peak current intensities of 2.75% (Chit + TiO₂ + 4HIS/GCE) and 4.30% (Chit + 4HIS/GCE), respectively, showing very good repeatability of responses at each modified electrode.

The reproducibility was examined by comparing the responses of six different modified electrodes prepared following the same experimental procedure. The relative standard deviations of the obtained current peak intensities were 2.78% at Chit + TiO₂ + 4HIS/GCE and 3.5% at Chit + 4HIS/GCE-modified electrodes, respectively.

The short-time stability of the studied modified electrodes was estimated by performing cyclic voltammograms during 25 cycles in 10^{-3} M DS, with a scan rate of 50 mV s⁻¹. The intensity of the peak was similar during the first 25 cycles, with a slight decrease in the anodic peak intensity of about 5% for all prepared electrodes.

The obtained results show that the developed nanocomposite-based modified electrodes had good repeatability, reproducibility, and stability toward the determination of DS.

3.4. Interferences Study

The ability of the prepared modified electrode to be selective for DS determination was evaluated by adding different concentrations of potential interfering compounds that might be present in real biological samples together with the analyte. Thus, 10^{-3} M glucose, citric acid, fructose, ibuprofen, paracetamol, or dopamine were added to a 10^{-5} M DS prepared in 0.025 M PB (pH 4.6), and the peak current intensities in the presence and absence of interference compounds were compared. The signal change, expressed in percent, was calculated as the ratio $(I_{\text{int+DS}} - I_{\text{DS}})/I_{\text{DS}}$, where I_{DS} is the peak current intensity for DS and $I_{\text{int+DS}}$ is the peak current intensity for DS in the presence of the interfering compound.

As seen in Figure 6, for all prepared modified electrodes, the signal change of less than 5% is probably due to the selectivity caused by the histidine side chains of the unfolded flagellin contained in all electrode matrices. However, the greatest values for the signal changes were recorded in the case of citric acid and glucose for all prepared electrodes, especially at the Chit + TiO₂ + 4HIS/GCE-modified electrode. This behavior is most likely caused by the presence of TiO₂ anatase nanoparticles in the sensitive electrode matrix, which offers a high active surface area.

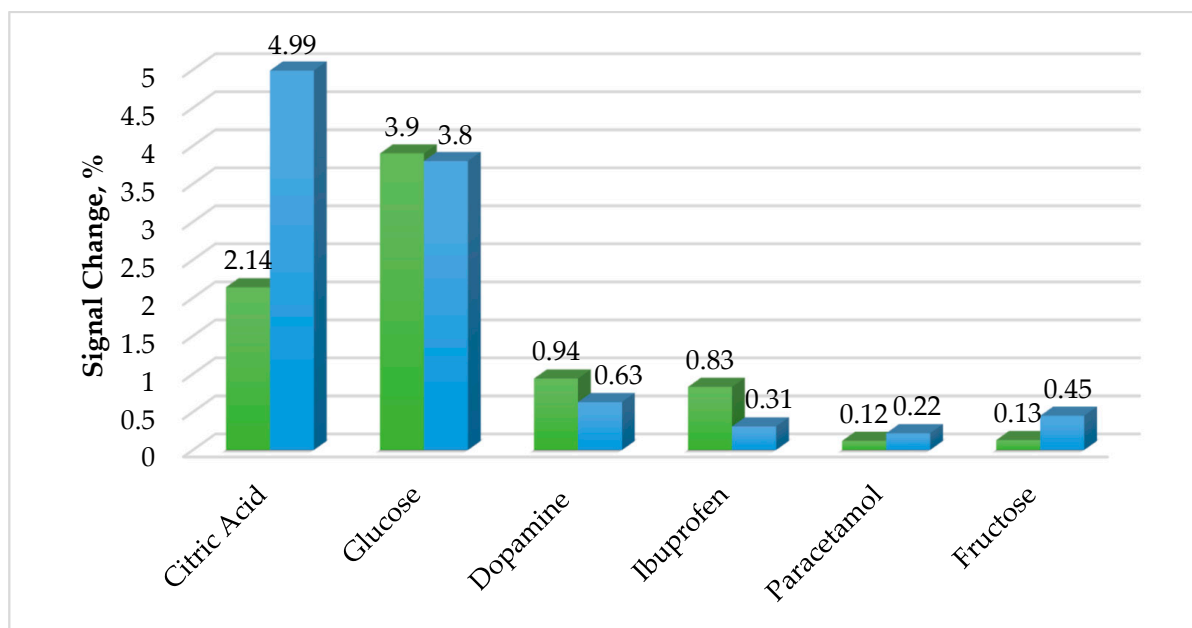


Figure 6. Interference studies at Chit + 4HIS/GCE (green) and Chit + TiO₂ + 4HIS/GCE (blue)-modified electrodes in the presence of 10^{−5} M DS in 0.025 M PB (pH 4.6) and 10^{−3} M of different contaminants.

These results suggest a good selectivity of the prepared electrodes, proving that the modified electrodes are a suitable technique for DS detection.

3.5. Determination of DS in the Pharmaceutical Sample and in the Wastewater Sample

The applicability of the developed modified electrodes was investigated for the determination of DS from pharmaceutical tablets containing 50 mg DS into an inert matrix of lactose monohydrate, povidone, corn starch, colloidal anhydrous silicon dioxide, magnesium stearate, and talc. In order to overcome the possible matrix effects, the standard addition method was performed. For this purpose, the tablet was crushed in an agate mortar, and a weighted quantity of powder was diluted in 100 mL 0.025 M PB (pH 4.6) to obtain a 1.57 μM DS final concentration and was sonicated for 10 min. A total of 10 μL of the drug solution was added to 10 mL of 0.025 M PB (pH 4.6), then additions of 10 and 25 μL of standard 10^{−4} M DS were performed and SWVs were recorded after each addition.

Figure 7A and Table 2 summarize the obtained results. It can be observed that the recovery was between 96–98.7% for all prepared modified electrodes, with the best results for the Chit + TiO₂ + 4HIS/GCE-modified electrode, proving that the presence of TiO₂ nanoparticles induces an enhanced behavior of the modifier matrix of the electrode. The obtained values are in good agreement with those indicated by the pharmaceutical producer. Due to this behavior, both Chit + 4HIS/GCE and Chit + TiO₂ + 4HIS/GCE-modified electrodes are sufficiently accurate and precise to be used for the determination of DS in biological samples.

Table 2. Comparative determination of DS in pharmaceutical products. Experimental conditions: see Figure 7A. Mean ± standard deviation of 3 measurements with different electrodes.

Type of Electrode	[DS]/μM Added	[DS]/μM Found	Recovery (%)	R/n
Chit + 4HIS/GCE	1.57	1.55 ± 0.63	98.72 ± 0.58	0.9964/6
Chit + TiO ₂ + 4HIS/GCE	1.57	1.51 ± 0.77	96.18 ± 0.4	0.9991/6

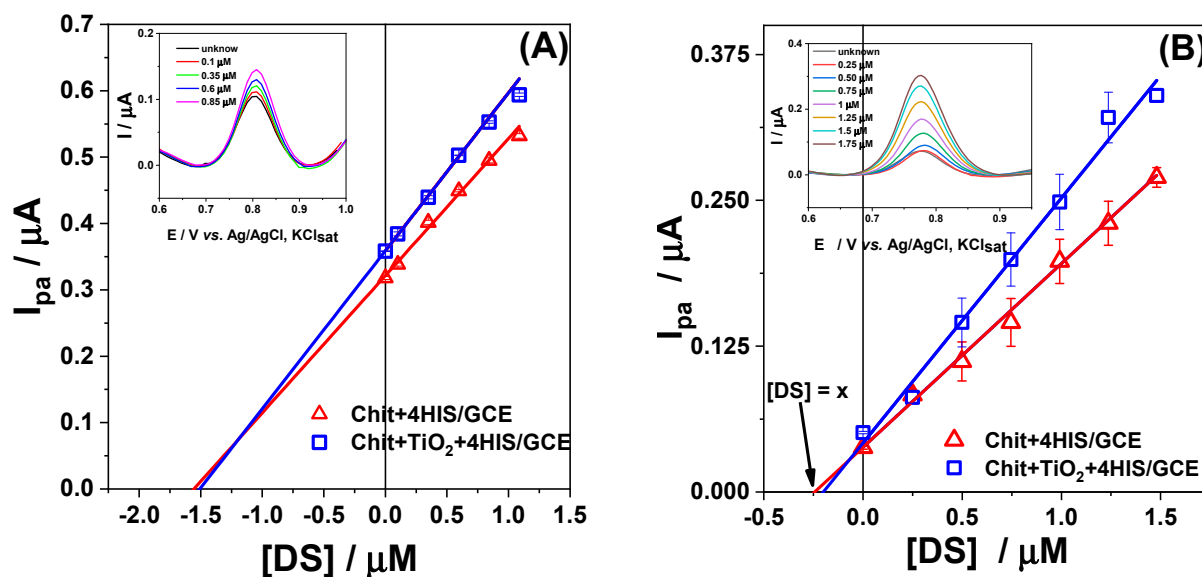


Figure 7. Standard addition plot obtained with a Chit + 4HIS/GCE (red) and Chit + TiO₂ + 4HIS/GCE (blue)-modified electrode, and the corresponding SWVs recorded at Chit + TiO₂ + 4HIS/GCE-modified electrode (inset) for DS determination in pharmaceutical product (A) and in wastewater (B) samples. Experimental conditions: frequency, 10 Hz; step potential, 0.01 V; amplitude, 0.01 V; starting potential, −0.4 V vs. Ag/AgCl, KCl_{sat}.

Another potential applicability of the prepared modified electrodes is the determination of DS concentration in wastewater samples, using the same standard addition method. No pretreatment of the wastewater samples was required. As previously described, the intensity of the peak increased linearly after each addition of aliquots of standard DS solution. The unknown concentration of DS was estimated by extrapolating the calibration curves (intersection with 0Y = 0 axis) from Figure 7B, and the obtained data are summarized in Table 3.

Table 3. Comparative determination of DS in wastewater sample. Experimental conditions: see Figure 7B. Mean ± standard deviation of 3 measurements with different electrodes.

Type of Electrode	SWV/ μM	HPLC/ μM	Relative Error/ %	RSD/ %
Chit + 4HIS/GCE	0.24 ± 0.026	0.19 ± 0.0018	20.83	3.53
Chit + TiO ₂ + 4HIS/GCE	0.20 ± 0.09		5	0.70

4. Conclusions

A newly modified electrode based on a matrix containing a novel bioengineered histidine-containing flagellin (4HIS) and TiO₂ nanoparticles immobilized with chitosan (Chit) polymer on the surface of GCE was prepared (Chit + TiO₂ + 4HIS/GCE) and characterized by electrochemical investigation techniques. TiO₂ nanoparticles in the polymeric matrix led to obtaining an active surface area that is double that of Chit + 4HIS/GCE. For diclofenac sodium detection, the Chit + TiO₂ + 4HIS/GCE-modified electrode had a LOD of less than 50% than the Chit + 4HIS/GCE-modified electrode, proving the beneficial effect of the presence of the TiO₂ anatase structure in the modifier matrix. The device was used for the determination of DF either from pharmaceutical or wastewater real samples, with good recoveries and results when compared with the standard methods of analysis. Compared to wild-type (histidine-free) flagellin-containing matrices, it can be concluded that the interaction of DS with the aromatic side chains of histidine plays an important role in the specific detection of DS.

Thus, based on the advantages of using TiO₂ in the electrode matrix, our work combines for the first time, to our knowledge, TiO₂ with bioengineered flagellin (4HIS) protein and improves the GCE-modified electrode performances (detection limit, linear range, selectivity, stability, etc.) for DS detection. Moreover, the obtained results, which are sufficiently accurate and precise, proved that the obtained modified electrodes can be used for the determination of DS in real samples.

Author Contributions: Conceptualization, J.S.H., G.L.T., C.I.F., I.G., H.J. and E.T.; methodology, J.S.H., G.L.T., C.I.F. and H.J.; software, J.S.H., G.L.T., C.I.F. and H.J.; validation, J.S.H., G.L.T. and C.I.F.; formal analysis, J.S.H., G.L.T., C.I.F., H.J., E.T. and É.T.; investigation, J.S.H. and É.T.; data curation, J.S.H., G.L.T., I.G. and J.S.H.; writing—original draft preparation, J.S.H., G.L.T., C.I.F., I.G., H.J. and E.T.; writing—review and editing, J.S.H., G.L.T., C.I.F., I.G., H.J. and E.T.; visualization, J.S.H., G.L.T., C.I.F. and H.J.; supervision, G.L.T., C.I.F. and I.G. All authors have read and agreed to the published version of the manuscript.

Funding: This research received no external funding.

Institutional Review Board Statement: Not applicable.

Informed Consent Statement: Not applicable.

Data Availability Statement: Data are contained within the article.

Acknowledgments: Juan Hidalgo acknowledges the Erasmus fellowship from Pannonia University (Veszprem, Hungary) for financing the research stay at “Babes-Bolyai” University (Cluj-Napoca, Romania). The authors thank Dorina Simedru for providing SEM measurements. Also, this work has been partially implemented by the TKP2021-NKTA-21 project with the support provided by the Ministry of Culture and Innovation of Hungary from the National Research, Development and Innovation Fund, financed under the 2021 Thematic Excellence Programme funding scheme.

Conflicts of Interest: The authors declare no conflict of interest.

References

1. Oaks, J.L.; Gilbert, M.; Virani, M.Z.; Watson, R.T.; Meteyer, C.U.; Rideout, B.; Shivaprasad, H.L.; Ahmed, S.; Jamshed, M.; Arshad, M.; et al. Diclofenac residues as the cause of vulture population decline in Pakistan. *Nature* **2014**, *427*, 630–633. [[CrossRef](#)] [[PubMed](#)]
2. EU. *Commission Implementing Decision (EU) 2015/495 of 20 March 2015 Establishing a Watch List of Substances for Union-Wide Monitoring in the Field of Water Policy Pursuant to Directive 2008/105/EC of the European Parliament and of the Council (Notified under Document C(2015) 1756)*; European Commission, Ed.; European Commission: Brussels, Belgium, 2015.
3. Simon, E.; Duffek, A.; Stahl, C.; Frey, M.; Scheurer, M.; Tuerk, J.; Gehrmann, L.; Konemann, S.; Swart, K.; Behnisch, P.; et al. Biological effect and chemical monitoring of Watch List substances in European surface waters: Steroidal estrogens and diclofenac—Effect-based methods for monitoring frameworks. *Environ. Int.* **2022**, *159*, 107033. [[CrossRef](#)] [[PubMed](#)]
4. Yilmaz, B. GC–MS determination of diclofenac in human plasma. *J. Chromatogr.* **2010**, *71*, 549–551. [[CrossRef](#)]
5. Borenstein, M.; Xue, S.; Cooper, S.; Tzeng, T. Sensitive capillary gas chromatographic-mass spectrometric selected ion monitoring method for the determination of diclofenac concentrations in human plasma. *J. Chromatogr. B* **1996**, *685*, 59–66. [[CrossRef](#)] [[PubMed](#)]
6. Elkady, E.F. Simultaneous determination of diclofenac potassium and methocarbamol in ternary mixture with guaifenesin by reversed-phase liquid chromatography. *Talanta* **2010**, *82*, 1604–1607. [[CrossRef](#)]
7. Bhupendra, L.K.; Kaphalia, S.; Kumar, S.; Kanz, M.; Treinen-Moslen, M. Efficient high-performance liquid chromatography/ultraviolet method for determination of diclofenac and 4'-hydroxy diclofenac in rat serum. *J. Chromatogr. B* **2006**, *830*, 231–237. [[CrossRef](#)]
8. Lee, H.S.; Jeong, C.K.; Choi, S.J.; Kim, S.B.; Lee, M.H.; Ko, G.; Sohn, D.H. Simultaneous determination of aceclofenac and diclofenac in human plasma by narrow bore HPLC using column-switching. *J. Pharm. Biomed. Anal.* **2020**, *23*, 775–781. [[CrossRef](#)]
9. Sparidans, R.W.; Lagas, J.S.; Schinkel, A.H.; Schellens, J.H.; Beijnen, J. Liquid chromatography–tandem mass spectrometric assay for diclofenac and three primary metabolites in mouse plasma. *J. Chromatogr. B* **2008**, *872*, 77–82. [[CrossRef](#)]
10. Bhushan, R.; Gupta, D.; Mukherjee, A. Liquid chromatographic analysis of certain commercial formulations for non-opioid analgesics. *Biomed. Chromatogr.* **2007**, *21*, 1284–1290. [[CrossRef](#)]
11. Botello, J.C.; Caballero, G.P. Spectrophotometric determination of diclofenac sodium with methylene blue. *Talanta* **1995**, *42*, 105–108. [[CrossRef](#)]
12. de Souza, R.L.; Tubino, M. Spectrophotometric determination of diclofenac in pharmaceutical preparations. *J. Braz. Chem. Soc.* **2005**, *16*, 1068. [[CrossRef](#)]

13. Garcia, Z.M.; Albero, M.I. Flow-injection spectrophotometric determination of diclofenac sodium in pharmaceuticals and urine samples. *J. Pharm. Biomed. Anal.* **1998**, *17*, 267–273. [[CrossRef](#)] [[PubMed](#)]
14. El-Didamony, A.M.; Amin, A.S. Adaptation of a color reaction for spectrophotometric determination of diclofenac sodium and piroxicam in pure form and in pharmaceutical formulations. *Anal. Lett.* **2004**, *37*, 1151–1162. [[CrossRef](#)]
15. de Micalizzi, Y.C.; Pappano, N.B.; Debattista, N.B. First and second-order derivative spectrophotometric determination of benzyl alcohol and diclofenac in pharmaceutical forms. *Talanta* **1998**, *47*, 525–530. [[CrossRef](#)] [[PubMed](#)]
16. Sastry, S.; Mohana Rao, A.R.; Prasad, N.V. Spectrophotometric analysis of diclofenac sodium and piroxicam and their pharmaceutical preparations. *Anal. Lett.* **1987**, *2*, 75–80. [[CrossRef](#)]
17. Arancibia, J.A.; Escandar, G.M. Complexation study of diclofenac with β -cyclodextrin and spectrofluorimetric determination. *Analyst* **1999**, *124*, 1833–1838. [[CrossRef](#)] [[PubMed](#)]
18. Jin, W.; Zhang, J. Determination of diclofenac sodium by capillary zone electrophoresis with electrochemical detection. *J. Chromatogr. A* **2000**, *868*, 101–107. [[CrossRef](#)] [[PubMed](#)]
19. Sarhangzadeh, K.; Khatami, A.A.; Jabbari, M.; Bahari, S. Simultaneous determination of diclofenac and indomethacin using a sensitive electrochemical sensor based on multiwalled carbon nanotube and ionic liquid nanocomposite. *J. Appl. Electrochem.* **2013**, *43*, 1217–1224. [[CrossRef](#)]
20. Karuppiah, C.; Cheemalapati, S.M.; Chen, S.M.; Palanisamy, S. Carboxyl-functionalized graphene oxide-modified electrode for the electrochemical determination of nonsteroidal anti-inflammatory drug diclofenac. *Ionics* **2014**, *21*, 231–238. [[CrossRef](#)]
21. Baghayeri, M.; Maleki, B.; Zarghani, R. Voltammetric behavior of tiopronin on carbon paste electrode modified with nanocrystalline Fe₅₀Ni₅₀ alloys. *Mater. Sci. Eng. C* **2014**, *44*, 175–182. [[CrossRef](#)]
22. Baghayeri, M.; Nazarzadeh Zare, E.; Mansour Lakouraj, M. A simple hydrogen peroxide biosensor based on a novel electromagnetic poly(p-phenylenediamine)@Fe₃O₄ nanocomposite. *Biosens. Bioelectron.* **2014**, *55*, 259–265. [[CrossRef](#)] [[PubMed](#)]
23. Vahedi, J.; Karimi-Maleh, H.; Baghayeri, M.; Sanati, A.L.; Khalilzadeh, M.A.; Bahrami, M. A fast and sensitive nanosensor based on MgO nanoparticle room-temperature ionic liquid carbon paste electrode for determination of methyl dopa in pharmaceutical and patient human urine samples. *Ionics* **2013**, *19*, 1907–1914. [[CrossRef](#)]
24. Goyal, R.N.; Chatterjee, S.; Agrawal, B. Electrochemical investigations of diclofenac at edge plane pyrolytic graphite electrode and its determination in human urine. *Sens. Actuat. B Chem.* **2010**, *145*, 743–748. [[CrossRef](#)]
25. Eteya, M.; Rounaghi, M.; Deiminiat, B. Fabrication of a new electrochemical sensor based on Au-Pt bimetallic nanoparticles decorated multi-walled carbon nanotubes for determination of diclofenac. *Microchem. J.* **2019**, *144*, 254–260. [[CrossRef](#)]
26. de Carvalho, R.C.; Bettsa, A.J.; Cassidya, J.F. Diclofenac determination using CeO₂ nanoparticle modified screen-printed electrodes—A study of background correction. *Microchem. J.* **2020**, *158*, 105258. [[CrossRef](#)]
27. Salahuddin, M.; Akhter, S.; Basirun, W.J.; Akhtaruzzaman, M.; Mohammed, M.A.; Rahman, N.M.M.A.; Salleh, N.M. Bio-synthesized copper nanoparticle decorated multiwall carbon nanotube-nano cellulose nanocomposite: An electrochemical sensor for the simultaneous detection of acetaminophen and diclofenac sodium. *Surf. Interfaces* **2022**, *34*, 102385. [[CrossRef](#)]
28. Naz, S.; Nisar, A.; Qian, L.; Hussain, S.; Karim, S.; Hussain, S.Z.; Liu, Y.; Sun, H.; Ur-Rahman, A.; Ahmad, M. Graphene Oxide Functionalized with Silver Nanoparticles and ZnO Synergic Nanocomposite as an Efficient Electrochemical Sensor for Diclofenac Sodium. *Nano Brief Rep. Rev.* **2021**, *16*, 2150139. [[CrossRef](#)]
29. Thiagarajan, S.; Rajkumar, M.; Chen, S. Nano TiO₂-PEDOT Film for the Simultaneous Detection of Ascorbic Acid and Diclofenac. *Int. J. Electrochem. Sc.* **2012**, *7*, 2109–2122. [[CrossRef](#)]
30. Hajjizadeh, A.; Jabbari, H.; Heli, A.; Movahedi, A.M.; Haghighi, S. Evaluation of the electrocatalytic properties of NiCo(OH)₂ composite modified electrodes. *Electrochim. Acta* **2007**, *53*, 1766–1774. [[CrossRef](#)]
31. Jankovics, H.; Szekér, P.; Tóth, E.; Balázs, K.; Lábadi, Z.; Saftics, A.; Kalas, B.; Fried, M.; Petrik, P.; Vonderviszt, F. Flagellin-based electrochemical sensing layer for arsenic detection in water. *Sci. Rep.* **2021**, *11*, 3497. [[CrossRef](#)]
32. Boumya, W.; Taoufik, N.; Achak, M.; Bessbousse, H.; Elhalil, A.; Barka, N. Electrochemical sensors and biosensors for the determination of diclofenac in pharmaceutical, biological and water samples. *Talanta* **2021**, *3*, 100026. [[CrossRef](#)]
33. Shrivastava, S.; Jadon, N.; Jain, R. Next-generation polymer nanocomposite-based electrochemical sensors and biosensors: A review. *Trends. Anal. Chem.* **2016**, *82*, 55–67. [[CrossRef](#)]
34. John, B. Polymer Nanocomposite-Based Electrochemical Sensors, and Biosensors. In *Nanorods and Nanocomposites*; InTech Open: London, UK, 2020. [[CrossRef](#)]
35. Postolović, K.S.; Stanić, Z. Chitosan/TiO₂ nanoparticles modified carbon paste electrode as a sensitive volt-ammetric sensor for the determination of diclofenac sodium as an anti-inflammatory drug. *Mater. Today Commun.* **2023**, *37*, 107416. [[CrossRef](#)]
36. Dias, G.V.; Joseane, C.; Bernardes, B.N.; Wesling, D.M.; Larissa, S.; Marques, C.R. Preparation, and electrochemical capacitance of high surface area TiO₂-RuO₂ aerogels. *Open Ceram.* **2021**, *8*, 100196. [[CrossRef](#)]
37. Huang, X.J.; Choi, Y.K. Chemical sensors based on nanostructured materials. *Sens. Actuat. B* **2007**, *122*, 659–671. [[CrossRef](#)]
38. Seracu, D. *Indreptar de Chimie Analitica (Tabele, Diagrame, Programme)*; Editura Tehnica: Bucuresti, Romania, 1989; p. 116, ISBN 973-3100-935.
39. Kashefi-Kheyabadi, L.; Mehrgardi, M.A. Design, and construction of a label-free aptasensor for electrochemical detection of sodium diclofenac. *Biosens. Bioelectron.* **2012**, *33*, 184–189. [[CrossRef](#)]
40. Deng, A.P.; Himmelsbach, M.; Zhu, Q.S.; Frey, S.; Sengl, M.; Buchberger, W.; Niessner, R.; Knopp, D. Residue analysis of the pharmaceutical diclofenac in different water types using ELISA and GCMS. *Environ. Sci. Technol.* **2003**, *37*, 3422–3429. [[CrossRef](#)]

41. Mohamed, M.; El-Wekil, A.; Saad, A.; Alkahtani, H.H.; Ali, R.H.; Mahmoud, A.M. Advanced sensing nanomaterials-based carbon paste electrode for simultaneous electrochemical measurement of esomeprazole and diclofenac sodium in human serum and urine samples. *J. Mol. Liq.* **2018**, *262*, 495–503. [[CrossRef](#)]
42. Abbas, A.; Bahiraei, A.; Madrakian, T. Gold nanoparticle/multi-walled carbon nanotube modified glassy carbon electrode as a sensitive voltammetric sensor for the determination of diclofenac sodium. *Mat. Sci. Eng. C* **2016**, *59*, 168–176. [[CrossRef](#)]
43. Labadi, Z.; Kalas, B.; Saftics, A.; Illes, L.I.; Jankovics, H.; Bereczk-Tompa, E.; Sebestyén, A.; Tóth, E.; Kakasi, B.; Moldovan, C.; et al. Sensing layer for Ni Detection in Water Created by Immobilization of Bioengineered Flagellar Nanotubes on Gold Surfaces. *ACS Biomater. Sci. Eng.* **2020**, *6*, 3811–3820. [[CrossRef](#)]
44. Bard, A.J.; Faulkner, L.R. *Electrochemical Methods: Fundamentals and Applications*, 2nd ed.; Wiley: New York, NY, USA, 2022; pp. 231, 591.
45. Killedar, L.; Ilager, D.; Shetti, N.P.; Aminabhavi, T.M.; Reddy, K.R. Synthesis of ruthenium doped titanium dioxide nanoparticles for the electrochemical detection of diclofenac sodium. *J. Mol. Liq.* **2021**, *340*, 116891. [[CrossRef](#)]
46. Shah, A.; Ullah, A.; Rauf, A.; Rehman, Z.; Shujah, S.; Shah, S.M. Detailed electrochemical probing of a biologically active isoquinoline. *J. Electrochem. Soc.* **2013**, *160*, H597. [[CrossRef](#)]
47. Honakeri, N.C.; Malode, S.J.; Kulkarni, R.M.; Shetti, N.P. Electrochemical behavior of diclofenac sodium at core-shell nanostructure modified electrode and its analysis in human urine and pharmaceutical samples. *Sens. Int.* **2020**, *1*, 100002. [[CrossRef](#)]
48. Nasraoui, S.; Ameer, S.; Al-Hamry, A.; Mounir, B.; Olfa Kanoun, A. Development of an Efficient Voltammetric Sensor for the Monitoring of 4-Aminophenol Based on Flexible Laser-Induced Graphene Electrodes Modified with MWCNT-PANI. *Sensors* **2022**, *22*, 833. [[CrossRef](#)]
49. Harvey, D. *Modern Analytical Chemistry*, 1st ed.; McGraw-Hill: Boston, MA, USA, 2000; p. 95.
50. Daizong, J.; Zhouyuanjing, S.; Zixiang, L.; Sze, S.L.; Jingwen, Z.; Tingkai, Z.; Zetao, C.; Xiongjie, Y.; Yanli, L.; Di, L.; et al. Smartphone-based square wave voltammetry system with screen-printed graphene electrodes for norepinephrine detection. *Smart Mater. Med.* **2020**, *1*, 1–9. [[CrossRef](#)]

Disclaimer/Publisher’s Note: The statements, opinions and data contained in all publications are solely those of the individual author(s) and contributor(s) and not of MDPI and/or the editor(s). MDPI and/or the editor(s) disclaim responsibility for any injury to people or property resulting from any ideas, methods, instructions or products referred to in the content.